Langmuir

Article

pubs.acs.org/Langmuir

Surface Shear Rheology of Saponin Adsorption Layers

Konstantin Golemanov,[†,‡] Slavka Tcholakova,[*,†] Nikolai Denkov,[†] Edward Pelan,[‡] and Simeon D. Stoyanov[‡,§,∥]

[†]Department of Chemical Engineering, Faculty of Chemistry and Pharmacy, Sofia University, 1 J. Bourchier Avenue, 1164 Sofia, Bulgaria

[‡]Unilever R&D, Vlaardingen, The Netherlands

[§]Laboratory of Physical Chemistry and Colloid Science, Wageningen University, 6703 HB Wageningen, The Netherlands

[∥]Department of Mechanical Engineering, University College London, Torrington Place, London WC1E 7JE, United Kingdom

Supporting Information

ABSTRACT: Saponins are a wide class of natural surfactants, with molecules containing a rigid hydrophobic group (triterpenoid or steroid), connected via glycoside bonds to hydrophilic oligosaccharide chains. These surfactants are very good foam stabiliziers and emulsifiers, and show a range of nontrivial biological activities. The molecular mechanisms behind these unusual properties are unknown, and, therefore, the saponins have attracted significant research interest in recent years. In our previous study (Stanimirova et al. *Langmuir* **2011**, *27*, 12486−12498), we showed that the triterpenoid saponins extracted from *Quillaja saponaria* plant (Quillaja saponins) formed adsorption layers with unusually high surface dilatational elasticity, 280 ± 30 mN/m. In this Article, we study the shear rheological properties of the adsorption layers of Quillaja saponins. In addition, we study the surface shear rheological properties of Yucca saponins, which are of steroid type. The experimental results show that the adsorption layers of Yucca saponins exhibit purely viscous rheological response, even at the lowest shear stress applied, whereas the adsorption layers of Quillaja saponins behave like a viscoelastic two-dimensional body. For Quillaja saponins, a single master curve describes the data for the viscoelastic creep compliance versus deformation time, up to a certain critical value of the applied shear stress. Above this value, the layer compliance increases, and the adsorption layers eventually transform into viscous ones. The experimental creep−recovery curves for the viscoelastic layers are fitted very well by compound Voigt rheological model. The obtained results are discussed from the viewpoint of the layer structure and the possible molecular mechanisms, governing the rheological response of the saponin adsorption layers.

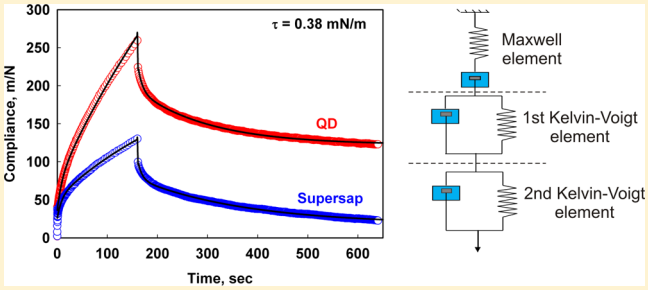

1. INTRODUCTION

Saponins are a class of natural surfactants found in more than 500 plant species.[1,2] They consist of (approximately) planar hydrophobic scaffold, connected via glycoside bonds with hydrophilic saccharide chains. The term "saponins" includes a great variety of compounds, differing in their structure and composition. The saponins are usually classified on the basis of (i) the type of hydrophobic group (triterpenoid, steroid, or steroid-alkaloid) and (ii) the number of sugar chains attached to it. The most common saponins have two sugar chains (bidesmosidic type), some have one sugar chain (monodesmosidic), and in rare cases, they have three sugar chains (tridesmosidic). Triterpenoid saponins are more proliferated in nature than are the steroid ones.

The diversity in the amphiphilic structures of the saponin molecules determines their rich physicochemical properties and biological activity. The high surface activity of saponins serves as a basis for their traditional use in food production,[3−7] and in some other industrial applications.[8−10] In recent years, various new applications have emerged in medicine,[11−18] food industry,[3,7,17,18] cosmetics,[9,19−21] and energy production.[22] Currently, saponins are used as foamers and emulsifiers in beer and soft drinks,[3,6] as solubilizing agents for vitamins[17] and minerals[18] in food additives, and as key ingredients in technologies for the decrease of cholesterol level in foods (fats, milk, butter).[3,4] These applications and the nontrivial properties of saponins have sparked recently increasing research activity in the areas of saponin extraction,[3] chemical and structural analysis,[1,23−25] and bioactivity.[7,10−15,26,27] An important open question in this context is what is the relation between the molecular structure of the saponins, on one side, and their bioactivity or physicochemical properties (micelle formation, solubilization capacity, surface activity, etc.), on the other side. A related question is whether some connection could be revealed between the physicochemical properties and

Received: May 26, 2012
Revised: July 18, 2012
Published: July 25, 2012

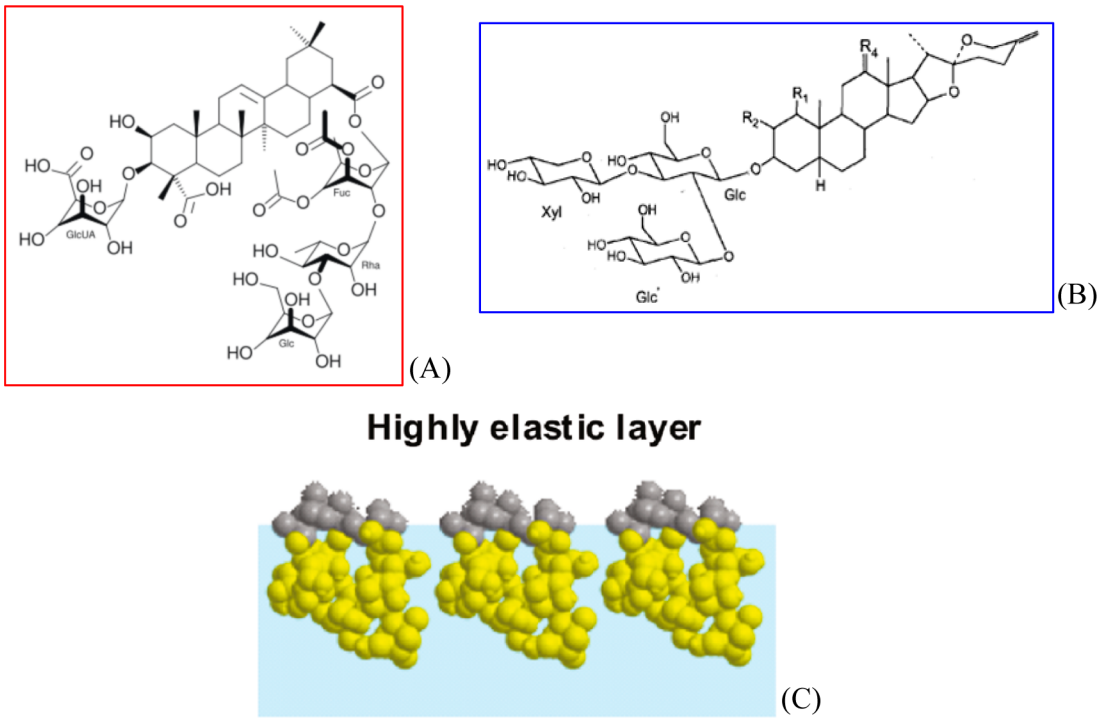

Figure 1. (A) General molecular structure of Quillaja saponins. (B) General molecular structure of Yucca saponins. Notation R_1–R_4 represents either H or different sugar groups. (C) Schematic presentation of the orientation of the Quillaja saponin molecules in the adsorption layer, as deduced from the area-per-molecule determination.[73] The dark-gray regions represent the hydrophobic triterpenoid rings, and the yellow regions represent the hydrophilic sugar residues.

the bioactivity of the specific saponins, due to the presence of some essential structural motifs in the saponin molecules.

In recent years, the interfacial rheology of a variety of surface-active species has been studied:[28,29] low molecular weight (LMW) surfactants,[29−32] proteins,[33−40] protein−surfactant mixtures,[38−40] synthetic polymers,[41,42] polysaccharides,[43−45] phospholipids,[46] lung surfactants,[47] and solid particles.[48−52] These studies have shown that the majority of the LMW surfactants have viscous rheological response of the adsorption layers, with very low shear elastic modulus (if any).[29,31,32] In contrast, proteins exhibit a complex visco-elastic behavior, which can be affected by the time of layer aging, heat pretreatment of the protein, type and concentration of surfactants present as additives, etc.[33−40] Some particle monolayers were shown to exhibit very high surface elasticity.[52] Thus, different types of surface adsorption layers have been observed, from the viewpoint of their rheological properties.

The surface properties of saponin layers are still poorly characterized, and, as a consequence, no information is available about the typical rheological behavior of the different saponins and how they compare to the other adsorbing species, mentioned above. Such knowledge is essential in the contexts of foam and emulsion formation and stabilization. For example, the surface rheological properties of the adsorption layers are known to have a significant impact on foam stability with respect to Ostwald ripenining[53−56] and water drainage,[57−59] as well as on the efficiency of bubble breakup into smaller bubbles during foaming.[60] Also, the surface rheological properties affect significantly the viscous friction in sheared foams,[53,54,61−63] and the friction between foams and confining solid walls, two processes that are important in foam extrusion and foam transportation along pipes and capillaries.[53,61,64] In addition, the surface properties of the surfactant solutions bring important information about the packing of the adsorbed molecules and the related intermolecular bonds in the adsorption layers.

Only a limited number of articles in the scientific literature is dedicated to studying the saponin adsorption layers.[65−74] Several authors[65,66,69,72,73] reported high surface elasticity and the presence of surface yield stress for saponin adsorption layers on the air−water interface. Thus, Joos et al.[69] tested the triterpenoid saponin "senegin", isolated from *Polygala Senega* L. plant,[75] and the steroid saponin "digitonin", extracted from *Digitalis purpurea* plant. These authors detected an irreproducible yield stress for the adsorption layers of the triterpenoid senegin, while no yield stress and much lower surface viscosity were found for the layer of the steroid digitonin. Blijdenstein et al.[72] studied commercial samples of saponins, extracted from *Quillaja Saponaria Molina* tree. These Quillaja saponins (QS) are of triterpenoid bidesmosidic type and are widely used as emulsifiers and foamers. By applying oscillatory shear deformation of QS adsorption layers, these authors[72] measured an elastic surface modulus that was much higher than the viscous one. In the same study,[72] it was demonstrated that the presence of QS in a foaming solution could decrease significantly the rate of bubble Ostwald ripening in foams.[72]

In our recent study,[73] we characterized several of the main surface properties of highly purified extracts of *Quillaja* saponins (QS), similar to those studied in ref 72. We found that, upon small dilatational surface deformation, the QS adsorption layers exhibit very high surface dilatational elasticity (280 ± 30 mN/m), much lower shear elasticity (26 ± 15 mN/m), and negligible true dilatational surface viscosity. The relaxation of QS adsorption layers, after small expansion or contraction of the layer, exhibited several characteristic times, which evidenced for the complexity of the relaxation processes involved. From surface tension isotherms, we determined the

dx.doi.org/10.1021/la302150j | *Langmuir* 2012, 28, 12071−12084

area per saponin molecule (~0.9 nm^2) and the preferred orientation of the molecules in the adsorption layers, laying with the triterpenoic scaffold parallel to the air−water interface with the sugar groups protruding toward the aqueous phase (see Figure 1C).

The current study is a direct continuation of our previous work[73] with the major aims being (1) to compare the basic surface shear rheological properties of two saponins of different types, the triterpenoid Quillaja saponins and the steroid Yucca saponins; (2) to characterize in detail the rheological behavior of the saponin adsorption layers, subject to shear deformation of type "creep−recovery"; (3) to describe the obtained data by an appropriate rheological model; and (4) to interpret the experimental results from the viewpoint of the possible molecular processes in sheared saponin adsorption layers.

This Article is organized as follows: In section 2 we describe the materials and methods used. Section 3.1 describes the experimental results from the rheological experiments. Section 3.2 describes the rheological model used for description of the experimental data, and the main results from the best fits of the data with this model. In section 3.3 we discuss these results from the viewpoint of the possible molecular mechanisms involved in layer deformation (shear and dilatational). Section 4 summarizes the main results and conclusions.

2. MATERIALS AND METHODS

2.1. Materials. Extracts from two plant species were studied: *Quillaja Saponaria Molina* (soap bark tree), and *Yucca Schidigera*. The Quillaja extract is a mixture of triterpenoid saponins with two sugar chains, whereas Yucca extract is a mixture of steroid saponins with one or two sugar chains (see Figure 1A,B).[76,77]

Two differently prepared Quillaja extracts and one Yucca extract were studied, all of them being products of the company Desert King, Chile. Quillaja Dry 100 (denoted as QD in the text) is a nonpreserved dried natural extract of *Quillaja Saponaria*, containing 25.6 wt % saponins. This extract is brown in color due to the presence of natural phenols and tannins, which are extracted together with the saponins. The second Quillaja sample, with commercial name Supersap, is a white powder with very high saponin purity, produced for pharmaceutical applications. This extract contains 91 wt % Quillaja saponins, while the rest is ~8 wt % moisture and traces of electrolytes and other organic ingredients. In our previous study,[73] we showed that the surface properties of QD extract are very similar to those of the purified Supresap sample, which indicates that the saponins are the most surface-active species in QD and dominate the properties of the formed adsorption layers. The third studied sample is a spray-dried natural extract of the *Mohave Yucca* plant (*Yucca Schidigera*), which contains 11% wt saponins.

All studied solutions were prepared to contain 0.5 wt % saponin with respect to the active ingredient, 10 mM NaCl (product of Sigma-Aldrich), and 0.1 g/L of the antibacterial agent NaN_3 (product of Riedel-de Haën). The used saponin concentration is well above the critical micelle concentration (CMC) for both types of saponins: by surface tension measurements, we determined CMC ≈ 0.025 wt % for the same Quillaja extracts,[73] and CMC ≈ 0.01 wt % was determined in the present study for the Yucca saponin sample. Therefore, the saponin concentration was at least 20 times above the CMC in all experiments described below.

2.2. Methods. The surface shear rheological properties of the adsorption layers were characterized with a Bicone tool, attached to a Bohlin Gemini rotational rheometer (Malvern Instruments, UK); see Figure 2. The radius of the tool is 28.1 mm, the inner radius of the vessel is 30 mm, and the gap between the tool and the inner wall of the vessel is 1.9 mm. A solution with volume ~2.6 mL was used to fill the vessel up to the bicone edge.

A small ring-shaped cup, filled with the studied solution, was fitted to the rod of the tool (not shown in the figure) to saturate the atmosphere in the measuring device with water vapors. The vessel was isolated from the ambient atmosphere with a solvent trap, which maintains high humidity and suppresses water evaporation from the studied solutions during the experiments. Care was taken to remove all air bubbles from the solution surface prior to the experiments, because such bubbles could compromise the measurements.

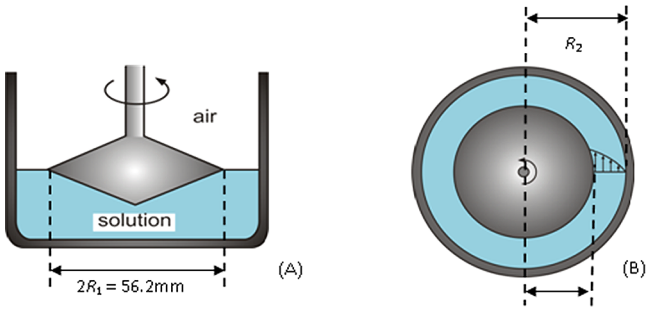

Figure 2. Bicone tool for interfacial shear rheological measurements. (A) Lateral view; (B) top view. The solution is poured to the edge of the tool. The distance between the edge of the tool and the wall of the vessel is r = 1.9 mm. R_1 is the radius of the bicone tool, and R_2 is the inner radius of the vessel. R_1 and R_2 are 28.1 and 30 mm, respectively. The distance between the lower tip of the bicone and the bottom of the vessel is 70 μm. The schemes are not drawn to scale.

The saponin solution, loaded in the vessel of the rheometer, was first thermostatted for 5 min at temperature T = 20 °C (controlled with Peltier element). Afterward, a preshear was performed with 120 rotations of the bicone for 1 min. After the preshear, the adsorption layer was left to age for different periods, before the actual rheological measurements were performed. The aging time was 0 (no aging), 2, 5, 10, or 20 min.

The aged adsorption layer was subjected to "creep−recovery" test (CRT). First, we applied constant shear stress, τ, for a given creep time, t_{CR}. Under the action of this creep stress, the monolayer was steadily deformed. The majority of the measurements were performed with creep time of t_{CR} = 40 s. For comparison, some experiments were performed with t_{CR} = 80 or 160 s. After the creep time expired, the stress was discontinued (τ = 0), and the recovery of the monolayer strain, caused by the visco-elastic nature of the layer, was monitored during the following 10 min.

During the test, the instrument records the angle of rotation of the bicone tool, $\theta(t)$, and the torque, $M(t)$, exerted by the sample on the tool, as functions of time, t. To calculate the rheological parameters of the adsorption layer, one has to perform an analysis of the data for $M(t)$ and $\theta(t)$ to calculate the shear strain, $\gamma(t)$, and the actual shear stress in the adsorption layer, $\tau(t)$. In this analysis, we considered the experimental setup as a 2D-Couette rheometer, an approach that requires some justification, as explained below.

The first issue is to calculate the shear strain in the adsorption layer for the used geometry. In reality, the strain across the gap is not constant, due to the curvature of the gap, and varies as follows:

$$\gamma(r) = \frac{2\theta R_1^2 R_2^2}{R_2^2 - R_1^2}\frac{1}{r^2};\ R_1 \le r \le R_2 \quad (1)$$

where R_1 = 28.1 mm is the radius of the bicone, and R_2 = 30 mm is the inner radius of the vessel. After substitution of the values of R_1 and R_2 in eq 1, one sees that the strain varies within ~12%, while varying r in the range $R_1 \le r \le R_2$. In our data interpretation, we neglected this variation of $\gamma(r)$ and assumed a homogeneous strain in the gap with a mean value, calculated from the approximation:[78]

$$\gamma = \frac{\theta(R_2 + R_1)}{2(R_2 - R_1)} \quad (2)$$

The second issue is to determine the actual shear stress in the adsorption layer, τ, from the measured torque. In the general case, the calculation of τ is nontrivial for two reasons. The first is due to the

dx.doi.org/10.1021/la302150j | Langmuir 2012, 28, 12071−12084

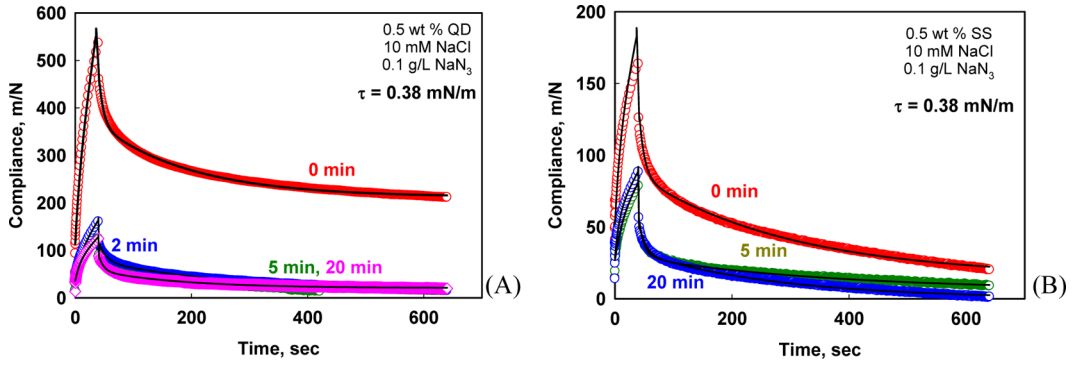

Figure 3. Compliance versus time (creep and recovery), at shear stress 0.38 mN/m. Before the test, the layer was aged for different periods of time: 0, 2, 5, 10, and 20 min. (A) Quillaja Dry; (B) Supersap. The symbols represent experimental results, whereas the curves are the best fits according to eqs 8 and 9. The creep time in these experiments is 40 s.

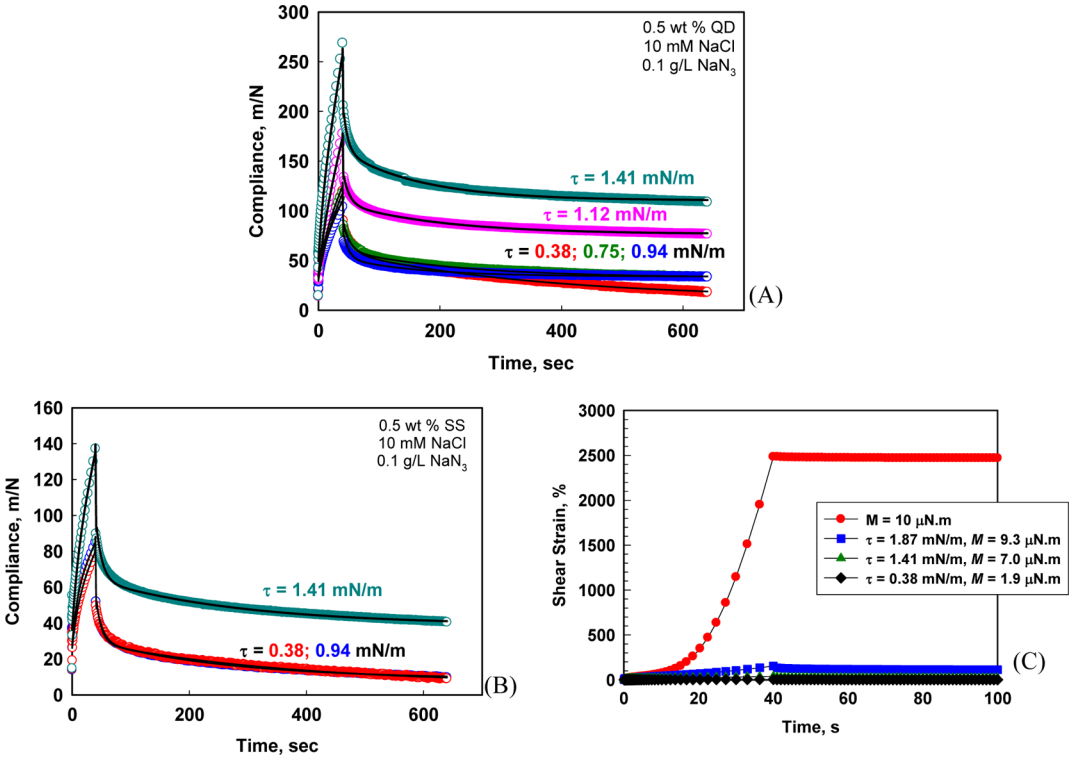

Figure 4. Compliance versus time (creep and recovery) at different values of the shear stress: (A) Quillaja Dry; (B) Supersap. In both graphs, the symbols represent experimental results, whereas the curves are the best fits according to eqs 8 and 9. (C) Shear strain versus time for QD; the red ● represent results obtained at $M = 10\ \mu$N m, whereas the other data are obtained at lower torques (1.9, 7.0, and 9.3 μN m, respectively). The elastic recoil at the lower torques, hardly seen in (C), is better represented in (A) where the ordinate scale is expanded. Much larger strain and no elastic recoil are seen at the highest torque in (C).

possible contribution to the torque of the friction between the lower surface of the bicone tool and the underlying liquid phase. We found that this contribution was negligible in the experiments in which viscoelastic layer properties were determined, because the rotation speed was rather low ($\sim 10^{-4}$ rad/s). We verified the latter statement by performing control experiments with pure water (no saponin in the solution and no adsorption layer on the air−water interface), at the same speed of tool rotation as in the experiments with saponins. The measured torque in these experiments was negligible (at least 100 times smaller), as compared to the experiments with saponins present.

Second, in the calculation of τ, one must analyze also the coupling between the flow in the deformed adsorption layer and the flow in the subsurface aqueous layer. This intimate coupling between the strain in the adsorption layer and the flow in the underlying liquid substrate could contribute to the measured torque and should be carefully analyzed, if it is significant.[79−81] The relative importance of this coupling can be estimated by considering the value of the dimensionless Boussinesq number, *Bo*, which compares the surface drag stress to the subsurface drag stress:

$$Bo = \frac{\mu_S (V/L_S)}{\mu (V/L_B)} \frac{P}{S} = \frac{\mu_S}{\mu} \frac{2L_B}{R_1 L_S} \tag{3}$$

In eq 3, μ_S is the surface viscosity of the adsorption layer, μ is the bulk viscosity of the solution, L_S and L_B are the characteristic length scales of the decay of the surface and bulk flows respectively, V is a characteristic velocity, $P = 2\pi R_1$ is the perimeter of the bicone, and $S \approx \pi R_1^2$ is the area of the bicone in contact with the bulk liquid.

In systems with high values of *Bo*, the subsurface drag can be neglected, and the measured torque is governed by the viscoelastic properties of the adsorption layer.[81] The numerical estimates showed that, for the systems and conditions used in our study ($L_S \approx 1.9$ mm

dx.doi.org/10.1021/la302150j | *Langmuir* 2012, 28, 12071−12084

and $L_B \geq 70\ \mu$m), the Boussinesq number is very high when the layers exhibited viscoelastic behavior, which allows us to neglect the contribution of the subsurface drag to the measured torque. In the experiments probing the viscoelastic layer properties, we thus estimate $Bo > 1500$. Thus, we can conclude that the torque in our experiments is created predominantly by the actual surface stress in the viscoelastic adsorption layers. This allows us to calculate this stress directly from the torque:

$$\tau = \frac{M}{2\pi R_1^2} \tag{4}$$

In the experiments performed at relatively high torques, $M > 10\ \mu$N m, the adsorption layers had a purely viscous response (see section 3.1). In these experiments, the rate of strain of the layers was much higher, while the layer viscosity was much lower, and, therefore, the corresponding Boussinesq number was also much lower. One could calculate the true surface viscosity of such layers after careful analysis of the coupling between the flow fields in the surface and subsurface layers.[79−81] However, we did not attempt such a quantitative analysis of these experimental data, because we are primarily interested in the viscoelastic behavior of the saponin layers at small strains.

For presenting the experimental results, we use the shear compliance of the layer, $J(t)$, defined as the ratio between the shear strain, $\gamma(t)$, and the applied shear stress, τ.

$$J(t) = \frac{\gamma(t)}{\tau} \tag{5}$$

3. EXPERIMENTAL RESULTS AND DISCUSSION

The experimental results from the creep−recovery experiments are described in section 3.1. Their interpretation with a rheological model is discussed in section 3.2. Discussion of the dynamic properties of saponin layers, from the molecular viewpoint, is presented in section 3.3.

3.1. Experimental Results. In the current section, we present the experimental results for the compliance, $J(t)$, as measured in the rheological tests described in section 2.2. Experiments with saponin adsorption layers formed from Quillaja Dry (QD), Supersap, and Yucca saponins were performed, and the effects of the following factors were studied: (1) aging time, (2) applied shear stress, (3) creep time, and (4) type of saponin. Symbols in the figures represent the experimental data, whereas the solid curves represent their fits by the compound Voigt model; see section 3.2 for the model definition and discussion of the results.

3.1.1. Effect of Aging Time. In Figure 3, we compare results for $J(t)$ in creep−recovery experiments, conducted after different periods of aging of the adsorption layers (after preshear) for Quillaja Dry (QD) and Supersap extracts. These results show that the compliance decreases steadily with the time of aging, t_A, in the first 5 min and remains almost the same at longer aging times, $t_A \geq 5$ min. In other words, the time required for formation of equilibrium adsorption layer of Quillaja saponins is ∼5 min at the used saponin concentration of 0.5 wt %. All experimental results, presented in the following sections, are obtained with adsorption layers aged for 5 min, unless otherwise specified.

No effect of aging time was observed for Yucca saponins, which means that these layers reach equilibrium configuration within seconds and do not change their properties in the following 20 min.

3.1.2. Effect of the Applied Shear Stress. In Figure 4A and B, we compare the results for $J(t)$, obtained with QD and Supersap extracts, at different applied stresses. For each of these samples, a single master curve was found to describe all results for $J(t)$ at low shear stress, $\tau \leq 0.94$ mN/m. However, at higher shear stress, $\tau > 0.94$ mN/m, we observed a steady increase of the compliance with the increase of the shear stress. Up to a certain shear stress, $\tau \approx 1.8$ mN/m, the rheological response is still viscoelastic; the total deformation is relatively small, and there is an elastic recoil after removal of the applied stress. Upon further increase of the applied stress, $\tau > 1.8$ mN/m, the deformation becomes much larger and the layer behaves like a viscous body; the deformation increases linearly with time in the entire creep period, and no elastic recoil is seen after the stress removal (see Figure 4C). These results indicate a significant restructuring in the adsorption layer and a qualitative change of its rheological properties in the range of applied stresses 0.94 mN/m $\leq \tau \leq$ 1.8 mN/m.

The adsorption layers from the Yucca saponins were found to behave as viscous bodies even at the lowest applied shear stress; see section 3.1.4 for the respective experimental data and their discussion.

3.1.3. Effect of the Creep Time for Layers of Quillaja Saponins. Figure 5 presents results for the dependence $J(t)$,

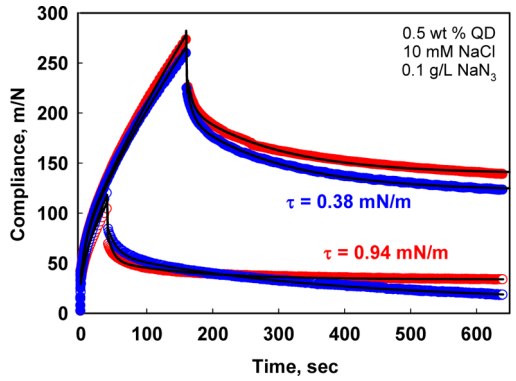

Figure 5. Compliance versus time (creep and recovery) for QD extract. Creep time: 40 s (empty symbols) and 160 s (full symbols). τ = 0.38 mN/m (blue symbols) and τ = 0.94 mN/m (red symbols). The symbols represent experimental results, whereas the curves are the best fits according to eqs 8 and 9.

obtained with QD adsorption layers, at different values of the applied stress and different creep times. Again, all results merge into a master curve, irrespective of the creep time and/or the applied shear stress, if the latter is below 0.94 mN/m. The compliance reached after 160 s of creep is more than 2 times higher than the compliance reached for 40 s creep. The latter result is a clear indication for a significant contribution of a steadily deformed viscous element to the overall rheological response of the layer; see section 3.2 for the rheological model that describes these data.

3.1.4. Comparison of the Results Obtained with QD, Supersap, and Yucca Saponins. Figure 6A compares the compliance for QD and Supersap, measured at the same shear stress. The compliance is lower for Supersap; smaller deformation is observed at the same applied stress. We remind that Supersap is a highly purified saponin extract. Therefore, the lower compliance can be attributed to better packing and stronger intermolecular interactions in the adsorption layers formed from the highly purified saponin, as compared to QD, which contains additional (nonsaponin) surface-active substances.

In Figure 6B, we present results for the shear strain versus time, from the creep−recovery experiments with Yucca and

dx.doi.org/10.1021/la302150j | Langmuir 2012, 28, 12071−12084

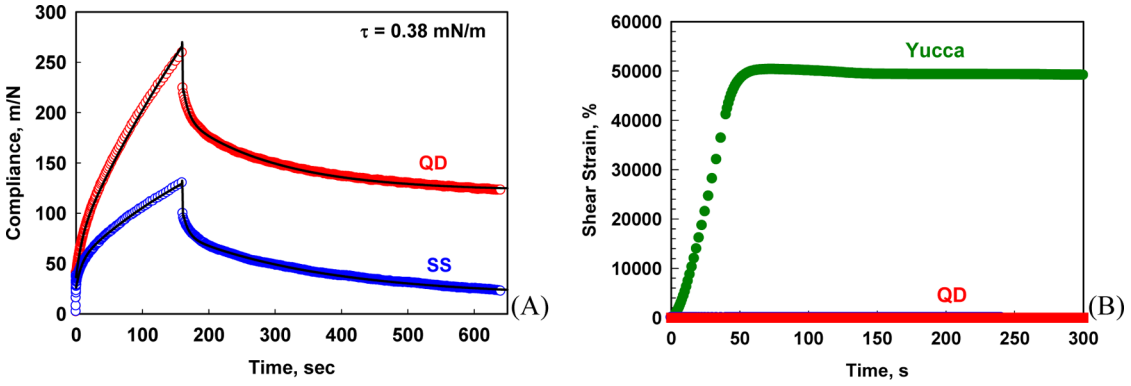

Figure 6. (A) Compliance versus time (creep and recovery) for QD (red ○) and SS (blue ○) extracts at the same shear stress, τ = 0.38 mN/m. (B) Shear strain versus time (creep and recovery) for Yucca extract (green symbols) as compared to QD extract, at the same torque M = 1.86 μN m. The symbols represent experimental results, whereas the curves are the best fits according to eqs 8 and 9. The rheological response for QD, which cannot be seen in (B), is represented in (A), where the same data for QD are shown at expanded ordinate scale.

QD, at the same (relatively low) torque, M = 1.86 μN m. As seen from the figure, the deformation of the Yucca layer is orders of magnitude larger, in comparison to the Supersap and QD layers. Furthermore, the Yucca layer exhibits no elasticity and shows very low viscosity; both quantities are below the sensitivity of the used rheometer and cannot be measured reliably. Approximate estimates showed that the surface yield stress of the Yucca layers is below 0.3 mN/m and their surface viscosity is very low. Thus, we see that the Yucca adsorption layers behave as purely viscous bodies even at very low shear stresses, at which the Quillaja saponin layers behave as viscoelastic bodies.

3.2. Interpretation of the Experimental Results for Quillaja Saponins with Rheological Model. The results described so far allow us to outline the following physical picture for the adsorption layers of Quillaja saponins. During the first 5 min after the performed preshear, the saponin molecules rearrange on the surface and form a structure that (almost) does not evolve further with aging time. The applied stress does not affect significantly the intrinsic layer structure up to a certain critical stress ($\tau \approx$ 0.94 mN/m), and the layer response is viscoelastic. The decrease of the compliance, observed at higher shear stress, indicates a loss of the intrinsic layer structure, involving significant molecular rearrangement and breakup of some intermolecular bonds in the adsorption layer. Upon further increase of the shear stress ($\tau >$ 1.8 mN/m), the layer structure is disturbed heavily, and, as a result, it behaves as a viscous body without elastic response.

In this section, we describe the results for the viscoelastic behavior of the Quillaja saponin layers (QD and Supersap) with an appropriate rheological model. We tested a number of viscoelastic models, and we chose the one that provided a reasonable description of the experimental data with minimum adjustable parameters.

3.2.1. Choice of Appropriate Rheological Model for Description of the Experimental Data. We considered four linear viscoelastic models: those of Maxwell, Kelvin, Burgers, and the compound Voigt model. Schematic representation of these models is given in Figure 7 and in Figure S1 in the Supporting Information.

For a creep−recovery experiment, the Maxwell model predicts an immediate initial jump in the compliance, J, followed by a linear increase of J during the creep period, and an instantaneous jump of J after stress removal (without gradual relaxation). However, in our experiments, we observe a nonlinear increase of $J(t)$ during the creep period and significant slow relaxation after removal of the applied stress, two features that evidence that Quillaja saponin layers do not behave as a simple Maxwell body upon shear.

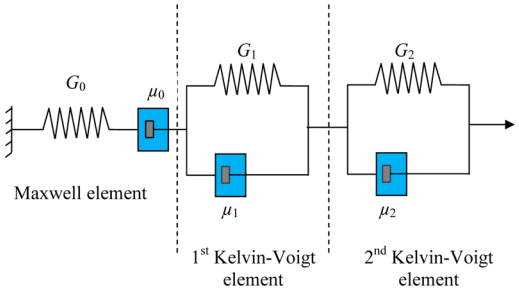

Figure 7. Schematic presentation of the compound Voigt model, consisting of one Maxwell and two Kelvin elements. Our experiments showed that two of the elastic moduli were equal for the studied Quillaja saponin layers, $G_0 = G_1$. Therefore, the experimental data for the creep and recovery periods were simultaneously fitted with compound Voigt model, containing five independent adjustable parameters.

According to the Kelvin model, the deformation should attain a constant value (plateau) after a certain creep time. In the recovery regime, no instantaneous decrease in J or residual deformation is expected, whereas we observed both features in our experiments. This comparison shows that Quillaja saponin layers do not behave as a Kelvin body as well.

The Burgers rheological model is composed of Kelvin and Maxwell elements, connected sequentially; see Figure S1-(C).[82−84] According to this model, the compliance during the creep stage of the deformation is described by the equation:[82]

$$J(t) = \frac{1}{G_0} + \frac{1}{G_1}\left[1 - \exp\left(-\frac{t}{\lambda_1}\right)\right] + \frac{t}{\mu_0} \quad (6a)$$

$$\lambda_1 = \frac{\mu_1}{G_1} \quad (6b)$$

where G_0 and μ_0 are the elastic modulus and viscosity in the Maxwell element, G_1 and μ_1 are those in the Kelvin element, and λ_1 is the related characteristic relaxation time of the creep deformation. The compliance during recovery, J_R, is governed by the expression:[82]

dx.doi.org/10.1021/la302150j | Langmuir 2012, 28, 12071−12084

$$J_R(t) = \frac{t_{CR}}{\mu_0} + \frac{1}{G_1}\left[1 - \exp\left(-\frac{t_{CR}}{\lambda_1}\right)\right]\exp\left(-\frac{t - t_{CR}}{\lambda_1}\right)$$

$$\text{at } t > t_{CR} \tag{7}$$

where t_{CR} is the time of creep. According to this model, there should be a single relaxation time, λ_1, describing the results in both periods, of creep and recovery. Our data, however, clearly indicate the presence of two characteristic relaxation times during the recovery period of the experiment (see section 3.2.2 and Table 1 below for the respective data and explanations).

Table 1. Rheological Parameters Describing the QD and SS Layers at $t_A \geq 5$ min, $\tau \leq 0.94$ mN/m

parameter	QD	SS
G_0, mN/m	32 ± 5	40 ± 6
G_1, mN/m	31 ± 6	39 ± 6
G_2, mN/m	7 ± 3	7 ± 3
μ_0, Pa·m·s	2 ± 1	9 ± 5
μ_1, Pa·m·s	0.3 ± 0.1	0.3 ± 0.1
μ_2, Pa·m·s	1.3 ± 0.3	1.3 ± 0.3
λ_0, s	43 ± 17	260 ± 100
λ_1, s	10 ± 3	7 ± 3
λ_2, s	200 ± 90	200 ± 90

Such behavior, along with all other features of the rheological response mentioned so far, is consistent with the so-called "compound Voigt model".[83]

The compound Voight model is represented as one Maxwell and two Kelvin mechanical elements, connected sequentially; see Figure 7. According to this model, the compliance during creep obeys the equation:

$$J(t) = \frac{1}{G_0} + \frac{1}{G_1}\left[1 - \exp\left(-\frac{t}{\lambda_1}\right)\right] + \frac{1}{G_2}\left[1 - \exp\left(-\frac{t}{\lambda_2}\right)\right] + \frac{t}{\mu_0} \tag{8}$$

and during recovery, by the equation:

$$J_R(t) = \frac{t_{CR}}{\mu_0} + \frac{1}{G_1}\left[1 - \exp\left(-\frac{t_{CR}}{\lambda_1}\right)\right]\exp\left(-\frac{t - t_{CR}}{\lambda_1}\right) + \frac{1}{G_2}\left[1 - \exp\left(-\frac{t_{CR}}{\lambda_2}\right)\right]\exp\left(-\frac{t - t_{CR}}{\lambda_2}\right) \text{ at } t > t_{CR} \tag{9}$$

where G_2, μ_2, and $\lambda_2 = \mu_2/G_2$ are the elastic modulus, viscosity, and relaxation time of the second Kelvin element, respectively.

In Figure 8, we present results for the creep and recovery periods, obtained with QD layer. The curves represent fits by the Burgers model and by the compound Voigt model. One sees that both models describe well the creep part of the experiments; however, the recovery part is described only by the compound Voigt element, which contains two relaxation times.

Let us clarify unambiguously that all of our experimental data showed the presence of two relaxation times in the second period of the creep−recovery experiments; see Figures 3−8. This observation means that we need (at least) two Kelvin elements in the rheological model to describe these relaxations,

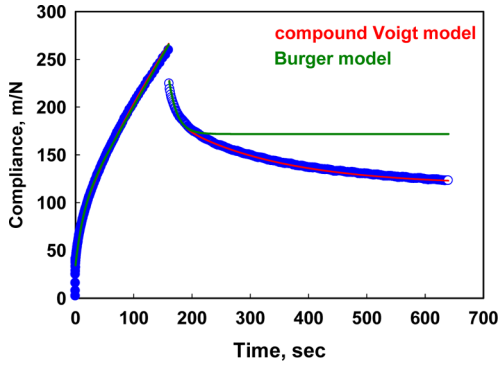

Figure 8. Creep and recovery of the compliance for QD extract, τ = 0.94 mN/m, t_A = 5 min, t_{CR} = 160 s. Fit with compound Voigt model (red curve) and with Burgers model (green curve).

because the Maxwell element relaxes instantaneously during the recovery period and cannot be used to explain the observed data. On the other hand, the observed jumps in the compliance at the beginning and at the end of the creep period mean that we need to include a spring from a Maxwell model to describe these data. The presence of residual compliance at the end of the recovery period means also that we need a dash-pot in a Maxwell model to describe this residual deformation. Summarizing, the simplest possible rheological model that can describe the two consecutive stages of the experiments with the Quillaja saponins in the viscoelastic regime of deformation is the compound Voigt model, which includes three elements; see Figure 7. As explained below, from the interpretation of the experimental data, we found that two of the elasticities in this model (of the Maxwell and one of the Kelvin elements) are equal in the frame of our accuracy, $G_0 \approx G_1$. Therefore, the data were eventually interpreted with compound Voigt model containing five independent parameters.

Let us note that we tested also several other rheological models, based on fractional derivatives.[84] However, following a similar series of arguments, as described above, and some numerical simulations, we found that we need a rheological model containing at least five independent parameters (Burger's model with fractional derivative) to describe our experimental data. Because no significant simplification of the rheological model has been achieved by using fractional derivatives, and because the physical interpretation of the linear models is more transparent (see section 3.3), we will not discuss below the rheological models, based on fractional derivatives.

3.2.2. Description of the Experimental Data for Quillaja Saponins by Compound Voigt Model. Both parts of the curves, creep and recovery, were simultaneously fitted by eqs 8 and 9, respectively, by using the Mathematica 8.0 package. From the best fit to the experimental data, the values of the six adjustable parameters were determined. It should be mentioned that the values of μ_0, G_2, and λ_2 can be determined accurately only when the relaxation is sufficiently long (600 s for the results reported below). If the relaxation is shorter, these three parameters cannot be separated reliably.

The values of the shear elasticities, as functions of the aging time, as determined from the experimental data for the QD sample, at τ = 0.94 mN/m and τ = 0.38 mN/m, are compared in Figure S2 in the Supporting Information. One sees that the values of G_0 and G_1 are always the same in the frame of our experimental accuracy. The most probable explanation of this

dx.doi.org/10.1021/la302150j | Langmuir 2012, 28, 12071−12084

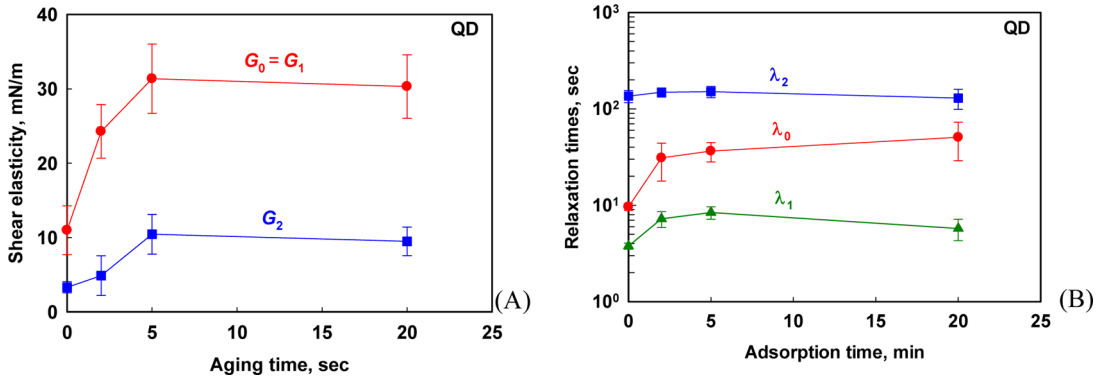

Figure 9. (A) Shear elasticities and (B) relaxation times as functions of aging time, as determined from the best fits to the experimental data from creep−recovery experiments, performed at τ = 0.94 mN/m with saponin adsorption layer from QD extract.

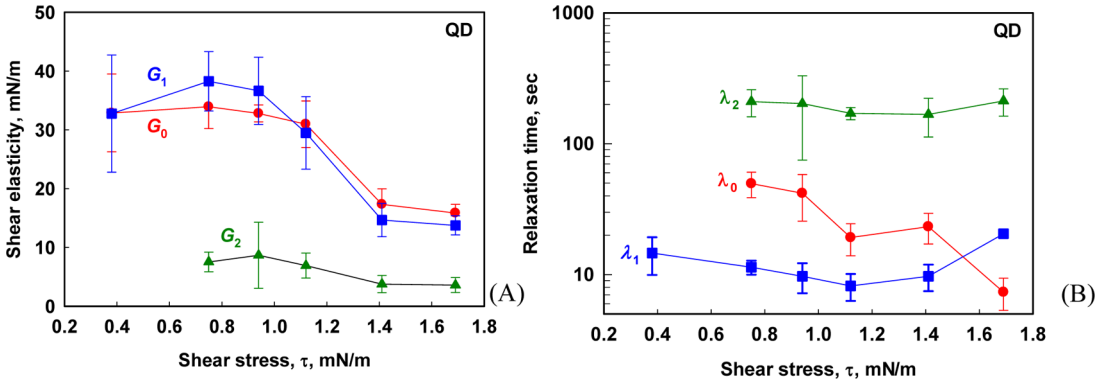

Figure 10. (A) Shear elasticities and (B) relaxation times as functions of the applied stress, determined from the best fits to the experimental data from creep−recovery experiments, performed with 5 min aged layers from QD extract.

coincidence in the values of G_0 and G_1 is that these two elasticities are coupled by their molecular origin; see section 3.3 for possible mechanistic explanation. To decrease the number of free adjustable parameters, in the following considerations, we set $G_0 = G_1$ in our model.

The dependence of G_0 and G_2 on the aging time for QD adsorption layer is shown in Figure 9A. One sees that both elasticities, G_0 and G_2, increased with the aging time during the first 5 min and remained constant afterward up to 20 min. At all aging times, the value of G_0 is approximately 3 times higher than the value of G_2. For the equilibrium layer ($t_A \geq 5$ min), $G_0 \approx 30$ mN/m, which is in very good agreement with the value, 26 ± 15 mN/m, determined from an entirely independent series of experiments, performed with the same saponins in the Langmuir trough.[73]

The relaxation times of the QD layers are shown in Figure 9B as functions of the aging time of the layer. One sees that the relaxation time associated with the Maxwell element, $\lambda_0 = \mu_0/G_0$, increased from 10 to 50 s with the aging time. The relaxation time associated with the first Kelvin element, $\lambda_1 = \mu_1/G_1$, is much shorter than λ_0 and increases from 3 to 8 s with the layer aging. Note that the elasticities of these two elements were found to be equal, $G_0 \approx G_1$, which means that the viscosity of the Maxwell element, μ_0, is 3−4 times higher than the viscosity of the first Kelvin element, μ_1. Interestingly, the relaxation time associated with the second Kelvin element remains almost constant, $\lambda_2 \approx 140$ s, for the entire process of layer aging. This qualitative difference in the behavior of the three relaxation times shows that they reflect different molecular processes in the adsorption layers. Thus, we can conclude that the compound Voigt model revealed three relaxation processes with characteristic times of ∼8, ∼50, and ∼140 s. In the performed creep−recovery experiments, only two of these relaxation times are directly seen (those associated with the two Kelvin elements), because the Maxwell element does not relax in this type of creep experiment.

The values of the determined shear elasticities are shown in Figure 10A, as functions of the applied stress. These experiments were performed with layers aged for 5 min. As explained above, G_0 and G_1 are equal in the frame of our experimental accuracy under all conditions studied. The value of G_2 is around 3 times lower than G_0 and G_1. One sees from Figure 10A that the values of G_0, G_1, and G_2 did not depend on the applied shear stress up to 0.94 mN/m, which means that the structure of the adsorption layer is not disrupted under low stresses. However, at higher shear stress, a significant decrease of all shear elasticities is observed. Further increase of the shear stress up to 2 mN/m leads to a complete disappearance of the layer elastic response (the layers start to behave as two-dimensional viscous bodies), which indicates a disruption of the initial elastic structure of the adsorption layer.

From Figure 10B, one sees that the relaxation times characterizing the Kelvin elements, λ_1 and λ_2, remain almost constant in the entire range of shear stresses, whereas a significant decrease of λ_0 is observed with the increase of the shear stress. This means that the largest changes in the adsorption layer upon aging and during shear at high velocity are associated with the Maxwell element in the used rheological model.

dx.doi.org/10.1021/la302150j | *Langmuir* 2012, 28, 12071−12084

The values determined with QD and Supersap adsorption layers are compared in Table 1. One sees that the values of G_0 and G_1 are higher by about 25% for the Supersap adsorption layer. The values of G_2 for QD and Supersap are practically the same in the frame of our accuracy. The viscosities of the Kelvin elements are also the same for both saponin extracts. However, a significant difference is observed for the two extracts in the values of μ_0 and λ_0. These two parameters are much higher for Supersap, as compared to QD (2 vs 9 Pa·m·s for μ_0 and 43 vs 260 s for λ_0). This means that the viscosity associated with the Maxwell element is much higher when pure saponin sample (Supersap) is used, instead of crude Quillaja extract (QD).

3.3. Possible Molecular Interpretation of the Results. *3.3.1. Comparison of Quillaja and Yucca Saponins.* As mentioned above, the Yucca extract contains a mixture of steroid saponins, whereas the Quillaja saponins are of triterpenoid type; see Figure 1. The different molecular structure (steroid vs triterpenoid) can lead to different packing of the molecules on the interface and to related different interactions between the adsorbed molecules, which could explain the different behavior of the studied saponins. The observed viscoelastic properties of the Quillaja saponin layers could be explained with tighter packing of the molecules in the adsorption layer and with formation of strong intermolecular bonds, most probably, multiple hydrogen bonds between the neighboring sugar residues. These interactions probably lead to the formation of a two-dimensional solid phase of packed saponin molecules in the Quillaja adsorption layers. The purely viscous behavior of the Yucca saponins, even at the lowest applied shear stresses, indicates for weaker interaction between the Yucca molecules, which are probably trapped in a fluid (most probably, liquid condensed) two-dimensional phase in the adsorption layer.

3.3.2. Molecular Interpretation of the Processes Detected in Deformed Adsorption Layers of Quillaja Saponins. As explained above, the experimental data in the current study demonstrate the presence of three relaxation times in the sheared layers of Quillaja saponins (QS), which should be associated with three different types of molecular rearrangements. Several relaxation times were detected also in our previous paper,[73] where we studied the relaxation processes after small expansion or compression of Supresap adsorption layers in Langmuir trough; see Table 2. All of these results evidence for a complex set of molecular processes, which appear in disturbed adsorption layers of QS.

Revealing the molecular interpretation of these observations, without having reliable information about the detailed layer structure, is an ambitious goal that would certainly involve speculative elements. Nevertheless, we decided to make an effort in this direction because this could help in the discussions of the rheological properties of such layers, in planning dedicated experiments for verification of the proposed physicochemical explanations, and in designing quantitative physical models of the studied phenomena.

Comparing the values of the various relaxation times in Table 2, we see that a short time of around 3 s appears only in the experiments involving rapid surface expansion.[73] As explained in ref 73, this fastest relaxation time is due to the process of actual adsorption of saponin molecules from the bulk micellar solution on the freshly formed air−water interface. As expected from this interpretation, such short relaxation time is not observed in the experiments involving shear and compression deformations of the layer, in which no new surface is created.

Let us consider now the longer relaxation times in Table 2. Upon shear and compression, we detect similar relaxation times of 7 and 11 s, respectively, whereas upon expansion we have a bit longer (but still in the same range) relaxation time of 19 s. Next, for shear deformations of Supresap layers, we have two similar relaxation times of $\lambda_0 \approx 260$ s and $\lambda_2 \approx 200$ s, which are comparable to the longest relaxation time after layer expansion, 180 s (without analogous relaxation time after layer compression). Finally, we detect a relaxation time of around 60 s after layer compression, which has no analogues in the other modes of surface deformation studied. As we describe below, these multiple relaxation times could be explained by assuming certain structure of the adsorption layers and an intimately related ensemble of molecular rearrangement processes.

First, we assume that the aged layer of Quillaja saponins is in a solid condensed state and contains multiple domains of relatively well-packed saponin molecules, separated by "weaker" (disordered) interdomain boundaries; see Figure 11. Each domain contains molecules oriented uniformly with respect to each other (to optimize their interaction energy), whereas the orientation of the molecules in the different domains is different, Figure 11B. Such a "domain" structure is a natural assumption for solid (two-dimensional) body with intrinsic

Table 2. Characteristic Relaxation Times of the Processes in Deformed Adsorption Layers of Quillaja Saponins (after Aging for 5 min)[a]

type of deformation	relaxation times, s			
shear		$\lambda_1 = 7 \pm 3$		$\lambda_0 = 260 \pm 100$ $\lambda_2 = 200 \pm 100$
compression		11 ± 1	62 ± 14	
expansion	2.7 ± 0.2	19 ± 1		180 ± 20

[a]The compression and expansion are made at 6% area deformation in Langmuir trough, with adsorption layers formed from 0.1 wt % Supersap solutions.[73] The characteristic times are grouped in the columns to be similar in value; see section 3.3.2 for explanations and discussion.

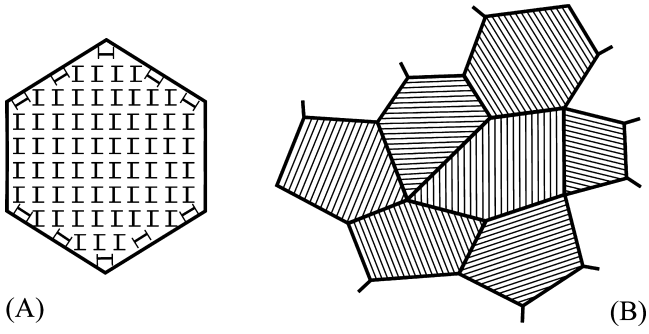

Figure 11. Schematic presentation of the assumed domain structure of the aged adsorption layers of Quillaja saponin. (A) Saponin molecules in each domain are packed in the appropriate orientation to maximize the intermolecular interactions. This favored orientation from the viewpoint of intermolecular interactions is schematically shown as aligned strings of molecules. (B) The various domains contain molecules of different orientations. The boundaries between the domains have higher energy (corresponding to excess linear energy) because the boundary molecules are interacting less favorably with their disordered neighbors.

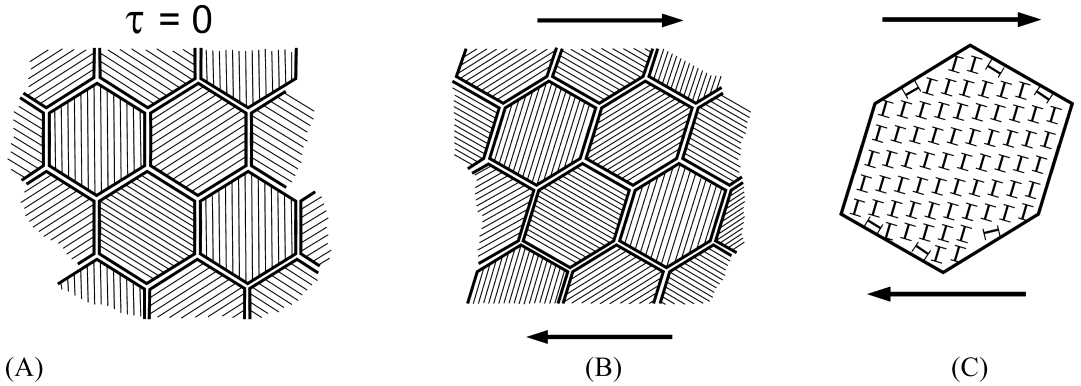

Figure 12. Schematic presentation of the domain perturbation (related to the immediate elastic response) under applied shear stress. The applied stress (B) elongates the domains in the shear direction, which leads to an increase of the total length of the domain boundaries, and (C) changes the orientation of the saponin molecules inside each domain, so that the intermolecular interactions are perturbed. Both processes lead to an increase of the internal free energy of the adsorption layer, as compared to the reference nonperturbed state shown in (A). For clarity of the graphical presentation, all domains are shown as regular in shape and size, which is probably not the case in reality.

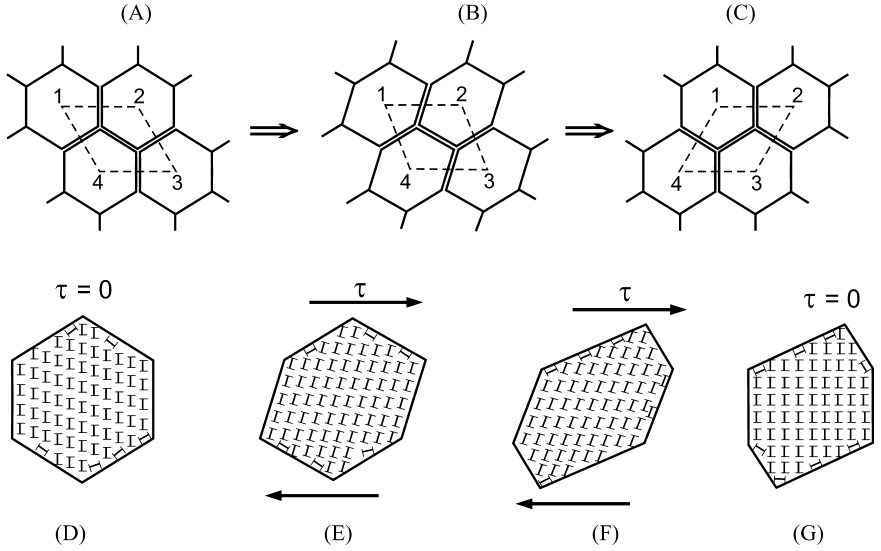

Figure 13. Schematic presentation of the processes, which are associated with the Maxwell and first Kelvin elements in the compound Voigt model. (A–C) Under applied stress, the domains can slide along each other in the shear direction; note the change of neighboring domains in (A) and (C). This process leads to irreversible translation of the domains and corresponds to the viscous dash-pot in the Maxwell element. (D–F) Under the same stress, the molecules at the domain boundaries could migrate, leading to plastic deformation along the shear direction, a process that increases the length of the domain boundaries and of the related domain linear energy. (G) After removal of the applied stress, the molecules inside the domains restore their favored molecular orientation; this process leads to elastic recoil and is coupled with a change of the domain shape. In the following period, the system could minimize the linear energy of the domains by a reverse migration of molecules along the domain boundaries; this reversible process is associated with a Kelvin element in the compound Voigt model.

visco-elasticity, as observed with Quillaja saponin layers. This structure is expected to form in the process of layer aging, through subsequent processes of domain nucleation and growth (e.g., after formation of a fresh solution surface, or after shearing at high shear rate of the adsorption layer when the layer structure is broken). In fact, a similar domain structure was observed with DPPC layers, as described recently in ref 85.

Note that the molecules that are well packed in the domain interiors are interacting favorably with their neighbors, while the molecules at the domain boundaries should have higher energy, because they interact with molecules of different orientations and are poorly packed. Therefore, the domain boundaries bring an excess of positive line energy with dimension [J/m]. If the boundaries of the domains are extended, as a result of shear deformation of the adsorption layer, the contribution of this line energy into the total energy of the adsorption layer should increase, because this contribution is proportional to the total length of the domain boundaries.

Let us consider now the changes in the layer structure upon deformation, and the possible molecular mechanisms that could lead to structural relaxation of the perturbed layers.

Under small shear stress, $\tau \leq 0.94$ mN/m, the domains in the QS adsorption layers get distorted, and the molecules inside the domains get reoriented along the shear direction; see Figure 12. The related deviation of the molecular orientation inside the domains from the equilibrium one (Figure 12C) and the extension of the domain boundaries (Figure 12B) are two processes that increase the layer energy. These processes are interrelated and very fast, so that they are detected as the elastic jump in the layer deformation, immediately after applying the

dx.doi.org/10.1021/la302150j | *Langmuir* 2012, 28, 12071–12084

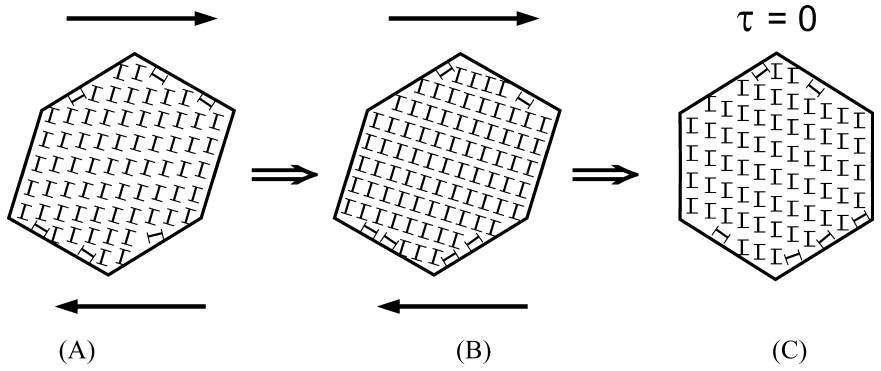

Figure 14. Schematic presentation of the process associated with the second Kelvin element in the compound Voigt model. (A) The applied stress reorients the molecules inside the domains, so that their most favored mutual orientation is perturbed. (B) By slow reorganization of the internal domain structure, the molecules in the stressed domains can restore their favored mutual orientation. (C) The removal of the external stress leads to rapid change of the molecule orientation in the opposite direction, a process that corresponds to the elastic recoil after stress removal. Slow reorganization of the molecules inside the domains (in the opposite direction) is needed to restore the favored molecular orientation, a process that can be associated with the second Kelvin element in the compound Voigt model.

external shear stress, and as the elastic recoil immediately after stress removal.

There are two obvious molecular mechanisms for relaxation of the distorted domain structure shown in Figure 12: (1) through sliding of the domains with respect to each other, under the action of the applied stress, along the weaker interdomain boundaries; see Figure 13A–C; and (2) through visco-plastic deformation of the domain boundaries, via migration of molecules along the domain sides, the domains get extended in the shear direction to comply with the applied stress; see Figure 13E,F. Note that, in the creep–recovery experiments described above, process (1) would lead to irreversible translation of the domains in the shear direction, under the action of the constant stress (i.e., this deformation of the layer is irreversible), whereas the second process would lead to extension of the domain boundaries, viz. to increase the linear energy of the domains. As a result, after removal of the external stress, the elastic recoil of the domains (due to reorientation of the molecules inside the domains leading to their most energetically favored mutual orientation) will result in domains with excess linear energy, which could relax via backward migration of boundary molecules (see Figure 13G); that is, process (2) is reversible. Therefore, we assume that process (1) is associated with the characteristic (relaxation) time $\lambda_0 = \mu_0/G_0$ (Maxwell element), whereas process (2) is associated with $\lambda_1 = \mu_1/G_1$ (Kelvin element), as defined in the rheological model described in section 3.2.

Note that the fast elastic deformation of the domains and the sliding of the domains along each other resemble to some extent the visco-elastic response of steadily sheared foams, where similar elastic deformation and sliding of the bubbles have been observed (see, e.g., ref 53). This analogy illustrates some of the processes under consideration here. However, it is rather limited, because the bubbles in foams have no internal structure, which is the case of the molecular domains in the adsorption layers (this structure leads to internal elasticity of the domains and more complex relaxation processes in the latter case).

The third relaxation time in the sheared layers, λ_2, might be associated with another process (3), which involves a rearrangement of the molecules inside the domains for restoring their most favored intermolecular orientation, so that the energy of molecular interactions inside the domains is minimized; see Figure 14. Such a process would require adjustment (translation and rotation) of the molecules inside the well packed domain interiors, and, therefore, one could expect this process to be slow, which agrees with the observed value $\lambda_2 \approx 200$ s. Note that upon removal of the external stress, the orientation of the packed molecules would be perturbed again (in the opposite direction, Figure 14C), and, therefore, this mechanism should be associated with a Kelvin element, as assumed in our rheological model for λ_2.

Let us see how these molecular processes would affect the layer behavior if small layer compression is applied, such as the deformations applied in ref 73. Upon compression, the area per molecule in the domain decreases and the domain boundaries shrink. The accumulated stress inside the compressed layer could be relaxed by desorption of molecules, a process that has no direct analogue in the other modes of deformation and could explain the relaxation time of 62 s, observed after layer compression only. In addition, molecular rearrangements at the domain boundaries are expected to occur, similar to process (2) in shear deformation, with a relaxation time close to λ_1. The lack of other relaxation times after layer compression could be explained with the preserved molecular orientation inside the domains and the lack of driving force for sliding of the domains with respect to each other, features that indicate that processes (1) and (3) are not involved in the relaxation of the compressed layers. In fact, some sliding of anisotropic domains could occur upon compression; however, due to the random orientation of the domains, we could expect cancelation of this effect, which explains why we do not detect it in our dilatational experiments (made with layers of relatively large areas, presumably comprising many domains with different orientations).

If we analyze now the layer expansion, the main trigger for the observed processes is the creation of a new air–water interface, which is expected to occur predominantly via widening the boundary regions between the domains (the "weak" spots in the layer). Now the expected modes of relaxation are: (1) true saponin adsorption from the underlying solution, with relaxation time of ~3 s; (2) adjustment of the molecules at the domain boundaries, associated with the relaxation time of 19 s (similar to λ_1); and (3) slow process of rearrangement of the molecules in the domains to achieve a better packing of all domains in the aging adsorption layer. The

dx.doi.org/10.1021/la302150j | *Langmuir* 2012, 28, 12071–12084

latter process is expected to occur with a characteristic time comparable to λ_2, as observed experimentally (180 vs 200 s).

The proposed structural model of the saponin layers could explain also the other observed trends in the obtained results. For example, the observed lower apparent viscosity, μ_0, and the related shorter relaxation time, λ_0, for the Quillaja Dry layers (see Table 1), which contain surface-active impurities, could be explained by assuming that these impurities are accumulated at the domain boundaries, because it is energetically less favored to include them in the domain interior, dominated by well-packed saponin molecules. Such an accumulation of impurities in the boundary regions would lead to weaker interactions between the various types of molecules in these regions, so that lower friction between the sheared domains is expected; as a result, the associated apparent viscosity μ_0 should be lower, whereas all other rheological parameters are expected to be similar to those of the Supersap layers, as observed experimentally (see Table 1).

This model allows us to explain qualitatively also why λ_2 does not vary significantly with the aging time, in contrast to λ_0 and λ_1; see Figure 9B. Indeed, λ_2 is associated with the packed molecular structure inside the domains, whereas λ_0 and λ_1 are associated with the boundaries of the domains. The aging process consists predominantly of the increase of the domain size and mutual structural adjustment of the growing domains, thus affecting strongly the detailed structure and composition of the domain boundaries and the related interdomain interactions, both processes being related to λ_0 and λ_1. The interior of the domains is less influenced by these aging processes, which could explain why λ_2 is weakly affected.

The above assumptions could explain also why the two elasticities, G_0 and G_1, have similar values, whereas the associated viscosities, μ_0 and μ_1, are very different. The driving force triggering processes 1 and 2 (and the associated elastic moduli) is the same, the overall domain deformation and the related extension of the domain boundaries, under the applied shear stress. However, the rate of relaxation via mechanisms (1) and (2) could be rather different, because the involved relaxation processes are very different from the viewpoint of molecular dynamics. Thus, the relaxation times and the related apparent viscosities are expected to be different, despite the similar values of the elastic moduli.

Thus, we see that the assumed "domain" structure of the layer and the related relaxation processes could explain qualitatively the main observations in the rheological experiments, performed with saponin adsorption layers.

4. MAIN RESULTS AND CONCLUSIONS

In this Article, we study the surface shear rheological properties of two extracts of Quillaja saponins and one extract of Yucca saponins. The Quillaja saponins are of triterpenoid type, whereas the Yucca saponins are of steroid type. The two Quillaja extracts differ in their purification levels: Supersap extract is a highly purified sample for pharmaceutical applications, whereas Quillaja Dry (QD) extract is a moderately purified sample for food and beverage applications.

The saponin adsorption layers on the air/water interface were subjected to creep−recovery experiments, and the obtained main results can be summarized as follows:

- At low shear stress, $\tau \leq 0.94$ mN/m, the adsorption layers of Quillaja saponins exhibit visco-elastic behavior. The layer properties during the creep and recovery stages can be described very well with a compound Voigt model, including one Maxwell, two Kelvin elements, and five independent parameters; see Figure 7. Other linear and fractional viscoelastic models were also tested, but they did not describe satisfactorily the data; see section 3.2.1.
- The parameters obtained for Supersap and QD samples are very similar, except for one of them; the viscosity of the Maxwell element is around 5 times lower for the QD sample. This similarity between the rheological models and parameters describing the Supersap and QD samples is a direct proof that the surface properties of the Quillaja saponin extracts are controlled predominantly by the saponin molecules, despite the presence of numerous other surface-active impurities (proteins, lipids) in the crude extract.
- The observed shear elasticity of the Quillaja layers is an indication for the formation of two-dimensional solid structure in the adsorption layer, at low shear stress. At higher shear stress, $\tau > 0.94$ mN/m, the elastic modulus of the Quillaja layers decreases, and at $\tau > 1.8$ mN/m the layers behave as purely viscous; see Figure 4. These results show that the internal "solid" structure of the layer is disrupted at high shear stress (and the related high shear rate of deformation).
- The observed complex rheological behavior of the Quillaja saponin layers is explained and discussed from the viewpoint of the possible layers structure, assumed to be composed of domains with different orientation of the packed saponin molecules, Figure 11. The related molecular relaxation processes are considered for the various modes of layer deformation (shear, compression, expansion); see section 3.3 and Figures 12−14.
- The studied adsorption layers of Yucca saponins behaved as purely viscous bodies even at the lowest shear stress we could apply; see Figure 6B.

The observed qualitative difference between the adsorption layers of the triterpenoid Quillaja saponins, which exhibited visco-elastic properties, and those of the steroid Yucca saponins with purely viscous behavior, is in agreement with the results by Joos et al.[69] These authors observed a similar trend with the triterpenoid saponin senegin and the steroid saponin digitonin. However, at this point, we do not have a sufficiently large pool of data with different saponins to generalize these trends to all members of the triterpenoid and steroid groups.

To the best of our knowledge, the compound Voigt model has not been used so far to describe the rheological properties of adsorption layers. Therefore, it would be of interest whether it could be applied to describe the complex rheological response of other molecular layers at fluid interfaces (e.g., of phospholipids, hydrophobin proteins, etc.).

■ ASSOCIATED CONTENT

Supporting Information

Figure with schematic presentation of (A) Maxwell, (B) Kelvin, and (C) Burger models.

Figure with shear elasticities as functions of aging time at two applied stresses, determined from the best fits to the experimental data from creep−recovery experiments, performedon layers from QD extract.

This material is available free of charge via the Internet at http://pubs.acs.org.

AUTHOR INFORMATION

Corresponding Author

*Phone: (+359-2) 962 5310. Fax: (+359-2) 962 5643. E-mail: sc@lcpe.uni-sofia.bg.

Notes

The authors declare no competing financial interest.

ACKNOWLEDGMENTS

We are grateful to Unilever R&D Vlaardingen, FP7 Project Beyond Everest, for support. K.G. is grateful to the Marie Curie Intra-European fellowship program.

REFERENCES

(1) Hostettmann, K.; Marston, A. *Saponins*; Cambridge University Press: New York, 1995.

(2) Vincken, J.-P.; Heng, L.; De Groot, A.; Gruppen, H. Saponins, classification and occurrence in the plant kingdom. *Phytochemistry* **2007**, *68*, 275.

(3) Guglu-Ustundag, Q.; Mazza, G. Saponins: Properties, applications and processing. *Crit. Rev. Food Sci. Nutr.* **2007**, *47*, 231.

(4) Micich, T. J.; Foglia, T. A.; Holsinger, V. H. Polymer-supported saponins: An approach to cholesterol removal from butteroil. *J. Agric. Food Chem.* **1992**, *40*, 1321.

(5) Ash, M.; Ash, I. *Handbook of Food Additives*; Synapse Information Resources Inc.: New York, 2002.

(6) Cheeke, P. R. Actual and potential applications of Yucca schidigera and Quillaja saponaria saponins in human and animal nutrition. *Proc.-Am. Soc. Anim. Sci.* **1999**, *E9*, 1−10.

(7) Oakenfull, D. Saponins in food - a review. *Food Chem.* **1981**, *6*, 19.

(8) Blunden, G.; Culling, M. C.; Jewers, K. Steroidal sapogenins: a review of actual and potential plant sources. *Trop. Sci.* **1975**, *17*, 139.

(9) Brown, R. The natural way in cosmetics and skin care. *Chem. Mark. Rep.* **1998**, *254*, FR8.

(10) Bomford, R.; Stapleton, M.; Winsor, S.; Beesly, J. E.; Jessup, E. A.; Price, K. R.; Fenwick, G. R. Adjuvancity and ISCOM formation by structurally diverse saponins. *Vaccine* **1992**, *10*, 572.

(11) Oakenfull, D. Soy protein, saponins and plasma cholesterol. *J. Nutr.* **2001**, *131*, 2971.

(12) Kim, S.-W.; Park, S.-K.; Kang, S.-I.; Kang, H.-C.; Oh, H.-J.; Bae, C.-Y.; Bae, D.-H. Hypocholesterolemic property of *Yucca schidigera* and *Quillaja saponaria* extracts in human body. *Arch. Pharm. Res.* **2003**, *26*, 1042.

(13) Ros, E. Intestinal absorption of triglycerides and cholesterol. Dietary and pharmacological inhibition to reduce cardiovascular risk. *Artherosclerosis* **2000**, *151*, 357.

(14) Kensil, C. R.; Mo, A. X.; Truneh, A. Current vaccine adjuvants: an overview of a diverse class. *Front. Biosci.* **2004**, *9*, 2972.

(15) Rao, V.; Sung, M.-K. Saponins as anticarcinogens. *J. Nutr.* **1995**, *125*, 717.

(16) Panagin Pharmaceuticals Inc. website: www.panagin.com/publications.html.

(17) Jenkins, K. J.; Atwal, A. S. Effects of dietary saponins on fecal bile acids and neutral sterols, and availability of vitamins A and E in the chick. *J. Nutr. Biochem.* **1994**, *5*, 134.

(18) Southon, S.; Wright, A. J. A.; Price, K. R.; Fairweather-Tait, S. J.; Fenwick, G. R. The effect of three types of saponin on iron and zinc absorption from a single meal in the rat. *Br. J. Nutr.* **1988**, *59*, 389.

(19) Indena S.p.A. website. Horse chestnut saponins. www.indena.com/pdf/horse_chestnut_saponins.pdf.

(20) Olmstead, M. J. Organic toothpaste containing saponin. U.S. Patent 6,485,711 B1, 2002.

(21) Bombardelli, E.; Morazzoni, P.; Cristoni, A.; Seghizzi, R. Pharmaceutical and cosmetic formulations with antimicrobial activity. U.S. Patent, Application 2001/0046525 A1, 2001.

(22) Das, D.; Panigrahi, S.; Misra, P. K.; Nayak, A. Effect of organized assemblies. Part 4. Formulation of highly concentrated coal-water slurry using a natural surfactant. *Energy Fuels* **1965**, *1008*, 22.

(23) Oleszek, W. Chromatographic determination of plant saponins. *J. Chromatogr., A* **2002**, *967*, 147.

(24) Oleszek, W.; Bialy, Z. Chromatographic determination of plant saponins - an Update. *J. Chromatogr., A* **2006**, *1112*, 78.

(25) Massiot, G.; Lavaud, C. Structural elucidation of saponins. *Stud. Nat. Prod. Chem.* **1995**, *15*, 187.

(26) Milgate, J.; Roberts, D. C. K. The nutritional and biological significance of saponins. *Nutr. Res. (N.Y.)* **1995**, *15*, 1223.

(27) Sparg, S. G.; Light, M. E.; van Staden, J. Biological activities and distribution of plant saponins. *J. Ethnopharmacol.* **2004**, *94*, 219.

(28) Sagis, L. M. C. Dynamic properties of interfaces in soft matter: Experiment and theory. *Rev. Mod. Phys.* **2011**, *83*, 1367.

(29) Kragel, J.; Derkatch, S. Interfacial shear rheology. *Curr. Opin. Colloid Interface Sci.* **2010**, *15*, 246.

(30) Miller, R.; Wustneck, R.; Kragel, J.; Kretzschmar, G. Dilatational and shear rheology of adsorption layers at liquid interface. *Colloids Surf., A* **1996**, *111*, 75.

(31) Erni, P.; Fischer, P.; Windhab, E. J. Sorbitan tristearate layers at the air/water interface studied by shear and dilatational interfacial rheology. *Langmuir* **2005**, *21*, 10555.

(32) Gavranovic, G. T.; Kurtz, R. E.; Golemanov, K.; Lange, A.; Fuller, G. G. Interfacial rheology and structure of straight-chain and branched hexadecanol mixtures. *Ind. Eng. Chem. Res.* **2006**, *45*, 6880.

(33) Murray, B. S. In *Proteins at Liquid Interfaces*; Mobius, D., Miller, R., Eds.; Elsevier: Amsterdam, 1998.

(34) Lucassen-Reynders, E. H.; Benjamins, J.; Fainerman, V. B. Dilatational rheology of protein films absorbed at fluid interfaces. *Curr. Opin. Colloid Interface Sci.* **2010**, *15*, 264.

(35) Freer, E. M.; Yim, K. S.; Fuller, G. G.; Radke, C. J. Interfacial rheology of globular and flexible proteins at the hexadecane/water interface: Comparison of shear and dilatation deformation. *J. Phys. Chem. B* **2004**, *108*, 3835.

(36) Dickinson, E. Absorbed protein layers at fluid interfaces. *Colloids Surf., B* **1999**, *15*, 161.

(37) Ariola, F. S.; Krishnan, A.; Vogler, E. A. Interfacial rheology of blood proteins absorbed to the aqueous-buffer/air interface. *Biomaterials* **2006**, *27*, 3404.

(38) Murray, B. S.; Dickinson, E. Interfacial rheology and dynamic properties of absorbed films of food proteins and surfactants. *Food Sci. Technol.* **1996**, *2*, 131.

(39) Kragel, J.; Derkatch, S. R.; Miller, R. Interfacial shear rheology of protein-surfactant layers. *Adv. Colloid Interface Sci.* **2008**, *144*, 38.

(40) Gunning, P. A.; Mackie, A. R.; Gunning, A. P.; Woodward, N. C.; Wilde, P. J.; Morris, V. J. Effect of surfactant type on surfactant-protein interactions at air-water interface. *Biomacromolecules* **2004**, *5*, 984.

(41) Noskov, B. A. Dilatational surface rheology of polymer and polymer/surfactant solutions. *Curr. Opin. Colloid Interface Sci.* **2010**, *15*, 229.

(42) Noskov, B. A.; Loglio, G.; Miller, R. Dilatational surface viscoelasticity of polyelectrolyte-surfactant solutions: Formation of heterogeneous absorption layers. *Adv. Colloid Interface Sci.* **2011**, *168*, 179.

(43) Arboleya, J.-C.; Wilde, P. J. Competitive adsorption of proteins with methylcellulose and hydroxypropyl methylcellulose. *Food Hydrocolloids* **2005**, *19*, 48.

(44) Erni, P.; Windhab, E. J.; Gunde, R.; Graber, M.; Pfister, B.; Parker, A.; Fischer, P. Interfacial rheology of surface-active biopolymers: Acacia. *Biomacromolecules* **2007**, *8*, 3458.

(45) Perez-Orozco, J. P.; Beristain, C. I.; Espinosa-Paredes, G.; Lobato-Calleros, C.; Vernon-Carter, E. J. Interfacial shear rheology of interacting carbohydrate polyelectrolytes at the water−oil interface using an adapted conventional rheometer. *Carbohydr. Polym.* **2004**, *57*, 45.

(46) Caro, A. L.; Nino, R. R.; Patino, J. M. R. The effect of pH on surface dilatational amd shear properties of phospholipid monolayers. *Colloids Surf., A* **2008**, *327*, 79.
(47) Wustneck, R.; Perez-Gil, J.; Wustneck, N.; Cruz, A.; Fainerman, V. B.; Pison, U. Interfacial properties of pulmonary surfactant layers. *Adv. Colloid Interface Sci.* **2005**, *117*, 33.
(48) Madivala, B.; Fransaer, J.; Vermant, J. Self-assembly and rheology of ellipsoidal particles at interfaces. *Langmuir* **2009**, *25*, 2718.
(49) Zang, D.; Langevin, D.; Binks, B. P.; Wei, B. Shearing particle monolayers: Strain-rate frequency superposition. *Phys. Rev. E* **2010**, *81*, 011604.
(50) Safouane, M.; Langevin, D.; Binks, B. P. Effect of particle hydrophobicity on the properties of silica particle layers at the air-water interface. *Langmuir* **2007**, *23*, 11546.
(51) Liggieri, L.; Santini, E.; Guzman, E.; Maestro, A.; Ravera, F. Wide-frequency dilatational rheology investigation of mixed silica nanoparticle-CTAB interfacial layers. *Soft Matter* **2011**, *7*, 7699.
(52) Xu, H.; Melle, S.; Golemanov, K.; Fuller, G. Shape and buckling transitions in solid stabilized drops. *Langmuir* **2005**, *21*, 10016.
(53) Denkov, N. D.; Tcholakova, S.; Golemanov, K.; Ananthapadmanabhan, K. P.; Lips, A. The role of surfactant type and bubble surface mobility in foam rheology. *Soft Matter* **2009**, *5*, 3389.
(54) Golemanov, K.; Denkov, N. D.; Tcholakova, S.; Vethamuthu, M.; Lips, A. Surfactant mixtures for control of bubble surface mobility in foam studies. *Langmuir* **2008**, *24*, 9956.
(55) Tcholakova, S.; Mitrinova, Z.; Golemanov, K.; Denkov, N. D.; Vethamuthu, M.; Ananthpadmanabhan, K. P. Control of bubble Ostwald ripening in foams by using surfactant mixtures. *Langmuir* **2011**, *27*, 14783.
(56) Saint-Jalmes, A. Physical chemistry in foam drainage and coarsening. *Soft Matter* **2005**, *2*, 836.
(57) Koehler, S. A.; Hilgenfeldt, S.; Weeks, E. R.; Stone, H. A. Drainage of single Plateau borders: Direct observation of rigid and mobile interfaces. *Phys. Rev. E* **2002**, *66*, 040601.
(58) Pitois, O.; Fritz, C.; Vignes-Adler, M. Hydrodynamic resistance of a single foam channel. *Colloids Surf., A* **2005**, *261*, 109.
(59) Ivanov, I. B. Effect of surface mobility on the dynamic behavior of thin liquid films. *Pure Appl. Chem.* **1980**, *52*, 1241.
(60) Golemanov, K.; Tcholakova, S.; Denkov, N. D.; Ananthapadmanabhan, K. P.; Lips, A. Bubble/drop breakup in steadily sheared foams and concentrated emulsions. *Phys. Rev. E* **2008**, *78*, 051405.
(61) Denkov, N. D.; Subraminian, V.; Gurovich, D.; Lips, A. Wall slip and viscous dissipation in sheared foams: Effect of surface mobility. *Colloids Surf., A* **2005**, *263*, 129.
(62) Denkov, N. D.; Tcholakova, S.; Golemanov, K.; Ananthapadmanabhan, K. P.; Lips, A. Viscous friction in foams and concentrated emulsions under steady shear. *Phys. Rev. Lett.* **2008**, *100*, 138301.
(63) Tcholakova, S.; Denkov, N. D.; Golemanov, K.; Ananthapadmanabhan, K. P.; Lips, A. Theoretical model of viscous friction inside steadily sheared foams and concentrated emulsions. *Phys. Rev. E* **2008**, *78*, 011405.
(64) Bretherton, F. P. The motion of long bubbles in tubess. *J. Fluid Mech.* **1961**, *10*, 166.
(65) Shorter, S. A. On surface separation from solutions of saponin, peptone, and albumin. *Philos. Mag.* **1909**, *17*, 560.
(66) Van Wazer, J. R. Some rheological measurements on the surface of saponin in water. *J. Colloid Sci.* **1947**, *2*, 223.
(67) Vochten, R.; Joos, P.; Ruyssen, R. Physico-chemical properties of acid saponins: Surface adsorption of sapoalbin. *Bull. Soc. Chim. Belg.* **1969**, *78*, 27.
(68) Vochten, R.; Ruyssen, R. Physico-chemical properties of acid saponins: The surface shear viscosity of adsorbed films of sapoalbin at the air-solution interface. *Bull. Soc. Chim. Belg.* **1969**, *78*, 331.
(69) Joos, P.; Vochten, R.; Ruyssen, R. The surface shear viscosity of mixed monolayers interaction between cholesterol and digitonin. *Bull. Soc. Chim. Belg.* **1967**, *76*, 601.
(70) Anton, N.; Bouriat, P. Different surface corrugations occurring during drainage of axisymmetric thin liquid films. *Langmuir* **2007**, *23*, 9213.
(71) Wojciechowski, K.; Piotrowski, M.; Popielarz, W.; Sosnowski, T. R. Short- and mid-termadsorption behaviour of *Quillaja* bark saponin and its mixtures with lysozyme. *Food Hydrocolloids* **2011**, *25*, 687.
(72) Blijdenstein, T. B. J.; de Groot, P. W. N.; Stoyanov, S. D. On the link between foam coarsening and surface rheology: Why hydrophobins are so different. *Soft Matter* **2010**, *6*, 1799.
(73) Stanimirova, R.; Marinova, K.; Tcholakova, S.; Denkov, N. D.; Stoyanov, S.; Pelan, E. Surface rheology of saponin adsorption layers. *Langmuir* **2011**, *27*, 12486.
(74) Piotrowski, M.; Lewandowska, J.; Wojciechowski, K. Bio-surfactant–protein mixtures: Quillaja bark saponin at water/air and water/oil interfaces in presence of β-lactoglobulin. *J. Phys. Chem. B* **2012**, *116*, 4843.
(75) Shimizu, Y.; Pelletier, S. W. Elucidation of the structures of the sapogenins of *Polygala senega* by correlation with medicagenic acid. *J. Am. Chem. Soc.* **1966**, *88*, 1544.
(76) Piacente, S.; Pizza, C.; Oleszek, W. Saponins and phenolics of Yucca Schidigera Roezl: Chemistry and bioactivity. *Phytochem. Rev.* **2005**, *4*, 177.
(77) Oleszek, W.; Sitek, M.; Stochmal, A.; Piacente, S.; Pizza, C.; Cheeke, P. Steroidal saponins of Yucca Schidigera Roezl. *J. Agric. Food Chem.* **2001**, *49*, 4392.
(78) Macosko, C. W. *Rheology: Principles, Measurements and Applications*; Wiley-VCH: New York, 1993.
(79) Oh, S. G.; Slattery, J. C. Disc and biconical interfacial viscometers. *J. Colloid Interface Sci.* **1978**, *67*, 516.
(80) Jiang, T. S.; Cheng, J. D.; Slattery, J. C. Nonlinear interfacial stress-deformation behavior measured with several interfacial viscometers. *J. Colloid Interface Sci.* **1983**, *7*, 96.
(81) Erni, P.; Fischer, P.; Windhab, E. J. Stress- and strain-controlled measurements of interfacial shear viscosity and viscoelasticity at liquid/liquid and gas/liquid interfaces. *Rev. Sci. Instrum.* **2003**, *74*, 4916.
(82) Steffe, J. F. *Rheological Methods in Food Process Engineering*; Freeman Press: New York, 1996.
(83) Mezger, T. G. *The Rheology Handbook*, 2nd ed.; Vincentz Network: Hannover, 2006.
(84) Mainardi, F. *Fractional Calculus and Waves in Linear Viscoelasticity: An Introduction to Mathematical Models*; Imperial College Press: London, 2010.
(85) Choi, S. Q.; Steltenkamp, S.; Zasadzinski, J. A.; Squires, T. M. Active microrheology and simultaneous visualization of sheared phospholipid monolayers. *Nat. Commun.* **2011**, *2*, 312.